Original Paper _____ *Forma*, **18**, 263–293, 2003

A Constructive Approach to Modelling the Tight Shapes of Some Linked Structures

E. L. STAROSTIN*

Bernoulli Institute for Mathematics, Swiss Federal Institute of Technology, CH-1015 Lausanne, Switzerland
E-mail address: star@mpipks-dresden.mpg.de

(Received December 12, 2002; Accepted November 27, 2003)

Keywords: Ideal Knot and Link, Borromean Rings, Tight Clasp

Abstract. A variational approach is used to find the shortest curves connecting two pairs of points. The curves are to be separated by a constant distance and they are confined to lie in two orthogonal planes. The method is applicable to constructing tight shapes of linked structures each component of which is known to be planar. Two particular examples are considered and explicit solutions are presented for the Borromean rings, and for two clasped pieces of a rope that provide the minimum of the centreline length for a fixed diameter of the cross-section. A concept of tight periodic structures is introduced and discussed.

1. Introduction

The notion of an ideal shape of a knot or link has emerged recently as a result of attempts to introduce a quantity that, first, is well-defined and, second, can be measured on a physical realization of the knotted structure (MOFFATT, 1990, 1996; KATRITCH *et al*., 1996; GROSBERG *et al*., 1996). The idea is to ascribe a uniform thickness to (closed) curve(s) embedded in space, and then to look for a configuration of the given topology that provides the minimal length-to-thickness ratio under the constraint of self-impenetrability. There is a hope that this ratio would give a unique number for every knot or link type, thus providing a new means of classification. A number of works have appeared where the properties of the ideal representations are shown to be related to the behaviour of physical systems such as DNA knots (STASIAK *et al*., 1996) and catenanes (links) (LAURIE *et al*., 1998) or chemical dissipative structures (MALEVANETS and KAPRAL, 1998).

Although some first results have been recently obtained in the theory of ideal knots and links (GONZALEZ and MADDOCKS, 1999; LITHERLAND *et al*., 1999; GONZALEZ *et al*., 2002; CANTARELLA *et al*., 2002), a surprising fact is that little is known about the shapes themselves. Proven analytical solutions known so far, include only links with the centrelines

*Current address: Max Planck Institute for Physics of Complex Systems, Nöthnitzer Str. 38, D-01187 Dresden, Germany.

made up of straight line intervals and circular arcs. No explicit closed-form description has been found of an ideal configuration with a fragment where the contact generates a one-to-one mapping of the points on the centrelines. A number of approximations have been computed by means of the numerical algorithms (both stochastic and deterministic) that discretize the centreline and represent it as a polygonal line (LAURIE, 1998; PIERAŃSKI, 1998). The work of these algorithms models the evolution of the shape as the length-to-thickness ratio decreases.

Here a new approach to construct extremal tight shapes is presented. Although its application is currently limited to links with planar centrelines, it has enabled non-obvious shapes to be described by explicit closed-form expressions. There is reason to believe that both the method and the examples will provide an insight into the general properties of the ideal knots and links.

2. A Constrained Variational Approach

Consider a curve $\boldsymbol{r}_1(\sigma) = (x_1(\sigma), y_1(\sigma), 0)$ of class C^2 in the xy-plane, σ being a parameter, $\sigma \in [0, \Lambda]$ (Fig. 1). Let $\boldsymbol{r}_2(\sigma) = (x_2(\sigma), d, z_2(\sigma))$ be another curve of class C^2 lying in the orthogonal plane $y = d$ and parametrized with the same σ. We assume that the curves $\boldsymbol{r}_1$ and $\boldsymbol{r}_2$ represent the centrelines of two pieces of an incompressible rope of constant diameter d. The rope pieces touch each other continuously so that, for every $\sigma_0 \in [0, \Lambda]$, the points $\boldsymbol{r}_1(\sigma_0)$ and $\boldsymbol{r}_2(\sigma_0)$ are the closest ones, i.e. the distance between them is equal to d. Without loss of generality we may set $d = 1$.

We are seeking shapes of the curves $\boldsymbol{r}_1$ and $\boldsymbol{r}_2$ connecting two pairs of points such that the sum of their lengths is minimal

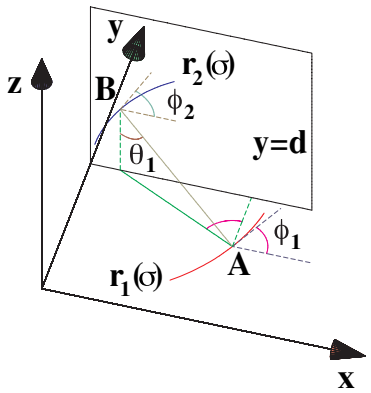

Fig. 1. The curves $\boldsymbol{r}_1(\sigma)$ and $\boldsymbol{r}_2(\sigma)$ lie in the orthogonal planes. The points $A = (x_1, y_1, 0)$ and $B = (x_2, d, z_2)$ belong to curves such that the chord AB is perpendicular to each of the curves with the distance AB is constant and equal to d.

$$L_1 + L_2 = \int_0^{\Lambda} \Phi\left(x_1', y_1', x_2', z_2'\right) d\sigma \to \min, \tag{1}$$

where $\Phi(x'_1,\ y'_1,\ x'_2,\ z'_2) = \sqrt{\left(x_1'\right)^2 + \left(y_1'\right)^2} + \sqrt{\left(x_2'\right)^2 + \left(z_2'\right)^2}$, the prime denoting the derivative with respect to σ.

The distance between the two curves should be constant, therefore we require

$$\boldsymbol{r}'_1 \cdot (\boldsymbol{r}_1 - \boldsymbol{r}_2) = 0, \quad \sigma \in [0, \Lambda], \tag{2}$$

and

$$\boldsymbol{r}'_2 \cdot (\boldsymbol{r}_1 - \boldsymbol{r}_2) = 0, \quad \sigma \in [0, \Lambda], \tag{3}$$

or, in coordinate form,

$$x'_1(x_1 - x_2) + y'_1(y_1 - 1) = 0, \tag{4}$$

and

$$x'_2(x_1 - x_2) - z'_2 z_2 = 0. \tag{5}$$

If we subtract Eq. (5) from Eq. (4) and then integrate the result, we obtain $\|\boldsymbol{r}_1 - \boldsymbol{r}_2\|^2 = \text{const}$.

It should be pointed out that, since we want to model the tight shape of a perfect rope, the curvature of the centreline may not exceed $2/d$. Nevertheless, no constraint on the curvature is explicitly included in the formulation of the variational problem. Instead, in the construction of the entire shape, we shall only choose extremal solutions that comply with the curvature constraint.

Thus, we look for a minimizer of the functional

$$\int_0^{\Lambda} \Psi\left(x_1, y_1, x_2, z_2, x_1', y_1', x_2', z_2', \lambda_1, \lambda_2\right) d\sigma \tag{6}$$

with

$$\begin{aligned}&\Psi\left(x_1, y_1, x_2, z_2, x_1', y_1', x_2', z_2', \lambda_1, \lambda_2\right)\\ &= \Phi\left(x_1', y_1', x_2', z_2'\right) - \lambda_1\left[x_1'\left(x_1 - x_2\right) + y_1'\left(y_1 - 1\right)\right] - \lambda_2\left[x_2'\left(x_1 - x_2\right) + z_2' z_2\right],\end{aligned}$$

where $\lambda_1(\sigma)$ and $\lambda_2(\sigma)$ are Lagrange multipliers associated with the pointwise constraints (2) and (3).

The corresponding Euler-Lagrange equations are

$$\frac{d}{d\sigma}\frac{\partial \Phi}{\partial x_1'} - \lambda_1'\left(x_1 - x_2\right) + x_2'\left(\lambda_1 + \lambda_2\right) = 0, \tag{7a}$$

$$\frac{d}{d\sigma}\frac{\partial\Phi}{\partial y_1'} - \lambda_1'(y_1 - 1) = 0, \tag{7b}$$

$$\frac{d}{d\sigma}\frac{\partial\Phi}{\partial x_2'} - \lambda_2'(x_1 - x_2) - x_1'(\lambda_1 + \lambda_2) = 0, \tag{7c}$$

$$\frac{d}{d\sigma}\frac{\partial\Phi}{\partial z_2'} + \lambda_2' z_2 = 0. \tag{7d}$$

We notice that

$$\frac{d}{d\sigma}\frac{\partial\Phi}{\partial x_1'} = -y_1'\kappa_1, \quad \frac{d}{d\sigma}\frac{\partial\Phi}{\partial y_1'} = x_1'\kappa_1, \quad \frac{d}{d\sigma}\frac{\partial\Phi}{\partial x_2'} = -z_2'\kappa_2, \quad \frac{d}{d\sigma}\frac{\partial\Phi}{\partial z_2'} = x_2'\kappa_2,$$

where

$$\kappa_1 = \frac{x_1'y_1'' - x_1''y_1'}{\left[(x_1')^2 + (y_1')^2\right]^{3/2}} \quad \text{and} \quad \kappa_2 = \frac{x_2'z_2'' - x_2''z_2'}{\left[(x_2')^2 + (z_2')^2\right]^{3/2}}$$

are the curvatures of the first and second curves, respectively. The system (7) then takes the form

$$-y_1'\kappa_1 - \lambda_1'(x_1 - x_2) + x_2'(\lambda_1 + \lambda_2) = 0, \tag{8a}$$

$$x_1'\kappa_1 - \lambda_1'(y_1 - 1) = 0, \tag{8b}$$

$$-z_2'\kappa_2 - \lambda_2'(x_1 - x_2) - x_1'(\lambda_1 + \lambda_2) = 0, \tag{8c}$$

$$x_2'\kappa_2 + \lambda_2' z_2 = 0. \tag{8d}$$

We can eliminate κ_1 (respectively κ_2) from Eqs. (8a) and (8b) (Eqs. (8c) and (8d)). The resulting equation is

$$x_1'x_2'(\lambda_1 + \lambda_2) = 0, \tag{9}$$

where we also took into account constraint (4) or (5).

Equation (9) is formally satisfied if at least one of the following equalities holds: a) $x_1 = x_{10} = \text{const}$, b) $x_2 = x_{20} = \text{const}$, c) $\lambda_1 + \lambda_2 = 0$.

In case a), Eq. (4) implies $y_1 = y_{10} = \text{const}$ which means that the fragment of the first curve reduces to a single point and the parametrization is singular. If the length of $\boldsymbol{r}_{2a}$ is non-zero, then the second curve $\boldsymbol{r}_{2a}$ may only be a circular arc of radius one with centre $(x_{10}, y_{10}, 0)$, which should belong to the plane $y = 1$. Thus, we have $\boldsymbol{r}_{1a} = \{(x_{10}, 1, 0)\}$, $\boldsymbol{r}_{2a} = \{(x_2 - x_{10})^2 + z_2{}^2 = 1, y_2 = 1\}$.

In case b), we have from Eq. (5) $z_2 = \text{const}$, and now the curve $\boldsymbol{r}_{2b}$ reduces to a point. The common parametrization is singular for the second curve. The situation is similar to case a) with the curves interchanged: the curve $\boldsymbol{r}_{1b}$ is a circular arc and $z_2 = 0$, i.e. $\boldsymbol{r}_{1b} = \{(x_1 - x_{20})^2 + (y_1 - 1)^2 = 1, z_1 = 0\}$, $\boldsymbol{r}_{2b} = \{(x_{20}, 1, 0)\}$.

Let $\boldsymbol{r}_{2a}$ and $\boldsymbol{r}_{1b}$ be complete circles. If $|x_{10} - x_{20}| = 1$, then $\boldsymbol{r}_{1a} \in \boldsymbol{r}_{1b}$ which implies $\boldsymbol{r}_{2b} \in \boldsymbol{r}_{2a}$ and we have the Hopf link which is known to be ideal as the solution of the Gehring link problem (CANTARELLA *et al.*, 2002, and references therein).

In the regular case we may reduce Eq. (9) to $\lambda_1 + \lambda_2 = 0$. Now we add Eqs. (8a) and (8c) with $\lambda_1 = -\lambda_2$ to get

$$y_1'\kappa_1 + z_2'\kappa_2 = 0. \tag{10}$$

Let us introduce an angle $\phi_1(\sigma)$ between the tangent to the curve $\boldsymbol{r}_1$ and the x-axis. Similarly, $\phi_2(\sigma)$ will be an angle between the tangent to $\boldsymbol{r}_2$ and the x-axis (see Fig. 1). Then

$$\sin\phi_1 = \frac{y_1'}{\sqrt{(x_1')^2 + (y_1')^2}}, \quad \cos\phi_1 = \frac{x_1'}{\sqrt{(x_1')^2 + (y_1')^2}}, \tag{11}$$

$$\sin\phi_2 = \frac{z_2'}{\sqrt{(x_2')^2 + (z_2')^2}}, \quad \cos\phi_2 = \frac{x_2'}{\sqrt{(x_2')^2 + (z_2')^2}}, \tag{12}$$

and

$$\kappa_1 = \frac{\phi_1'}{\sqrt{(x_1')^2 + (y_1')^2}}, \quad \kappa_2 = \frac{\phi_2'}{\sqrt{(x_2')^2 + (z_2')^2}}.$$

Equation (10) may be put in the form

$$\phi_1' \sin\phi_1 + \phi_2' \sin\phi_2 = 0,$$

which can be integrated to yield

$$\cos\phi_1 + \cos\phi_2 = C, \quad C = \text{const}, \quad |C| \le 2. \tag{13}$$

The integration constant C is specified by the tangents in a pair of corresponding points.

Equation (13) allows for the constant solutions $\phi_1 = \phi_2 = 0$ with $C = 2$, and $\phi_1 = \phi_2 = \pi$ with $C = -2$. These trivial solutions are just a pair of parallel straight lines.

With the help of Eqs. (4) and (5), we may eliminate the derivatives from Eqs. (11) and (12):

$$\sin\phi_1 = \pm\frac{\Delta x}{\sqrt{(\Delta x)^2 + (\Delta y)^2}}, \quad \cos\phi_1 = \mp\frac{\Delta y}{\sqrt{(\Delta x)^2 + (\Delta y)^2}},$$

$$\sin\phi_2 = \pm\frac{\Delta x}{\sqrt{(\Delta x)^2 + (\Delta z)^2}}, \quad \cos\phi_2 = \mp\frac{\Delta z}{\sqrt{(\Delta x)^2 + (\Delta z)^2}},$$

where we denote $\Delta x = x_2 - x_1$, $\Delta y = 1 - y_1$ and $\Delta z = z_2$. The property of constant distance between the two curves implies $(\Delta x)^2 = 1 - (\Delta y)^2 - (\Delta z)^2$, and we obtain from Eq. (13)

$$\mp\frac{\Delta y}{\sqrt{1-(\Delta z)^2}} \mp \frac{\Delta z}{\sqrt{1-(\Delta y)^2}} = C. \tag{14}$$

Let us now introduce an angle θ_1, $\theta_1 \in [0, \pi]$, between the vector $\boldsymbol{r}_2 - \boldsymbol{r}_1 = (\Delta x, \Delta y, \Delta z)$, $\|\boldsymbol{r}_2 - \boldsymbol{r}_1\| = AB$, and the z-axis. Since the tangent to the first curve at point A is orthogonal to AB, we can interpret the angles θ_1 and ϕ_1, $\phi_1 \in [0, 2\pi]$ as the spherical coordinates of the difference vector $\boldsymbol{r}_2 - \boldsymbol{r}_1$ (see Fig. 2):

$$\Delta x = -\sin\theta_1\sin\phi_1, \quad \Delta y = \sin\theta_1\cos\phi_1, \quad \Delta z = \cos\theta_1. \tag{15}$$

Conversely, we may define an angle θ_2, $\theta_2 \in [0, \pi]$, between the vector $\boldsymbol{r}_2 - \boldsymbol{r}_1$ and the $(-y)$-axis. The pair θ_2 and ϕ_2, $\phi_2 \in [0, 2\pi]$, may also serve as the spherical angles for the direction $\boldsymbol{r}_2 - \boldsymbol{r}_1$, because the tangent to the second curve at point B is always orthogonal to AB:

$$\Delta x = -\sin\theta_2\sin\phi_2, \quad \Delta y = \cos\theta_2, \quad \Delta z = \sin\theta_2\cos\phi_2. \tag{16}$$

We equate the expressions for the differences Δx and Δz from Eq. (15) and Eq. (16) and eliminate the angle θ_2 from the resulting equations. Then we are left with one equation for the angle θ_1 which can be written as

$$\sin^2\theta_1 = \frac{\sin^2\phi_2}{1 - \cos^2\phi_1\cos^2\phi_2}.$$

It is then possible to express the coordinates as functions of ϕ_1 and ϕ_2:

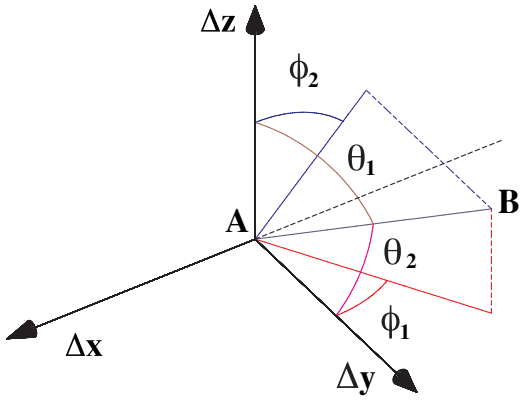

Fig. 2. Definition of spherical coordinates. The points *A* and *B* are the same as in Fig. 1. The projections of *AB* onto two coordinate planes are shown.

$$\Delta x(\phi_1,\phi_2) = -\varepsilon \frac{\sin\phi_1 \sin\phi_2}{\sqrt{1-\cos^2\phi_1 \cos^2\phi_2}}, \tag{17}$$

$$\Delta y(\phi_1,\phi_2) = \varepsilon \frac{\cos\phi_1 \sin\phi_2}{\sqrt{1-\cos^2\phi_1 \cos^2\phi_2}}, \tag{18}$$

$$\Delta z(\phi_1,\phi_2) = \varepsilon \frac{\sin\phi_1 \cos\phi_2}{\sqrt{1-\cos^2\phi_1 \cos^2\phi_2}}, \tag{19}$$

where $\varepsilon = \pm 1$. The last expressions suggest that $\Delta x(\phi_1, \phi_2) = \Delta x(\phi_2, \phi_1)$ and $\Delta y(\phi_1, \phi_2) = \Delta z(\phi_2, \phi_1)$.

There exist symmetries:

- $\phi_1 \to \pi - \phi_1$, $\phi_2 \to \phi_2 + \pi$, $\varepsilon \to \varepsilon$, $C \to -C$, $\Delta x \to -\Delta x$, $\Delta y \to \Delta y$, $\Delta z \to -\Delta z$ (rotation around the y-axis through π);
- $\phi_1 \to \phi_1 + \pi$, $\phi_2 \to \pi - \phi_2$, $\varepsilon \to \varepsilon$, $C \to -C$, $\Delta x \to -\Delta x$, $\Delta y \to -\Delta y$, $\Delta z \to \Delta z$ (rotation around the z-axis through π);
- $\phi_1 \to \phi_1$, $\phi_2 \to 2\pi - \phi_2$, $C \to C$, $\varepsilon \to -\varepsilon$, $\Delta x \to \Delta x$, $\Delta y \to \Delta y$, $\Delta z \to -\Delta z$ (reflection about the xy-plane).

Due to these symmetries, we may restrict ourselves, without loss of generality, to consideration of only one octant $\phi_1 \in [0, \pi/2]$, $\phi_2 \in [0, \pi/2]$ with $\varepsilon = 1$, where $\Delta x \le 0$, $\Delta y \ge 0$, $\Delta z \ge 0$.

Now we can choose either ϕ_1 or ϕ_2 as an independent variable, and, with the help of Eq. (13), we obtain the parametric representations of the coordinates of the curves $\boldsymbol{r}_1$ and $\boldsymbol{r}_2$:

$$x_1 - x_2 = \varepsilon \sqrt{\frac{1-\left(C-\cos\phi_1\right)^2}{1-\left(C-\cos\phi_1\right)^2\cos^2\phi_1}}\sin\phi_1, \tag{20}$$

$$y_1 = 1 - \varepsilon \sqrt{\frac{1-\left(C-\cos\phi_1\right)^2}{1-\left(C-\cos\phi_1\right)^2\cos^2\phi_1}}\cos\phi_1, \tag{21}$$

$$z_2 = \varepsilon \frac{\left(C-\cos\phi_1\right)\sin\phi_1}{\sqrt{1-\left(C-\cos\phi_1\right)^2\cos^2\phi_1}}, \tag{22}$$

and

$$x_1 - x_2 = \varepsilon \sqrt{\frac{1-\left(C-\cos\phi_2\right)^2}{1-\left(C-\cos\phi_2\right)^2\cos^2\phi_2}}\sin\phi_2, \tag{23}$$

$$y_1 = 1 - \varepsilon \frac{\left(C-\cos\phi_2\right)\sin\phi_2}{\sqrt{1-\left(C-\cos\phi_2\right)^2\cos^2\phi_2}}, \tag{24}$$

$$z_2 = \varepsilon \sqrt{\frac{1-\left(C-\cos\phi_2\right)^2}{1-\left(C-\cos\phi_2\right)^2\cos^2\phi_2}}\cos\phi_2. \tag{25}$$

We observe that when $\phi_1 = \pi/2$, then $x_1 - x_2 = \sqrt{1-C^2}$, $y_1 = 1$ and $z_2 = C$, i.e. the curve $\boldsymbol{r}_1$ intersects the plane of $\boldsymbol{r}_2$ at a right angle. Similarly, if $\phi_2 = \pi/2$, then $x_1 - x_2 = \sqrt{1-C^2}$, $y_1 = 1 - C$ and $z_2 = 0$, i.e. the second curve crosses the xy-plane orthogonally.

If $|C| > 1$, then each of the curves may cross the other plane non-orthogonally, namely, $\boldsymbol{r}_2$ crosses the xy-plane, when $\cos\phi_1 = \pm 1$, $\cos\phi_2 = C \mp 1$ and $\boldsymbol{r}_1$ crosses the plane $y = 1$, if $\cos\phi_1 = C \pm 1$, $\cos\phi_2 = \mp 1$.

Unfortunately, Eq. (20) gives us only the difference of the x-coordinates. We can find x_1 from the differential equation

$$\cot\phi_1 = \frac{\dfrac{dx_1}{d\phi_1}}{\dfrac{dy_1}{d\phi_1}}, \tag{26}$$

where ϕ_1 is treated as an independent variable and y_1 is assumed to be defined by Eq. (21). The last equation may be rewritten in an integral form as

$$x_1(\phi_1) = \int_{\phi_{10}}^{\phi_1} \cot\tilde{\phi}_1 \frac{dy_1}{d\tilde{\phi}_1} d\tilde{\phi}_1 + x_1(\phi_{10}). \tag{27}$$

Integration by parts yields

$$x_1(\phi_1) - x_1(\phi_{10}) = \cot\tilde{\phi}_1 y_1\left(\tilde{\phi}_1\right)\Big|_{\phi_{10}}^{\phi_1} + \int_{\phi_{10}}^{\phi_1} \frac{y_1\left(\tilde{\phi}_1\right)}{\sin^2\tilde{\phi}_1} d\tilde{\phi}_1. \tag{28}$$

Thus the x_1-coordinate is found as a quadrature. As to the x_2-coordinate, the above approach may be applied as well. This time we treat the relationship

$$\cot\phi_2 = \frac{\dfrac{dx_2}{d\phi_2}}{\dfrac{dz_2}{d\phi_2}} \tag{29}$$

as a differential equation for $x_2(\phi_2)$. Its integration gives

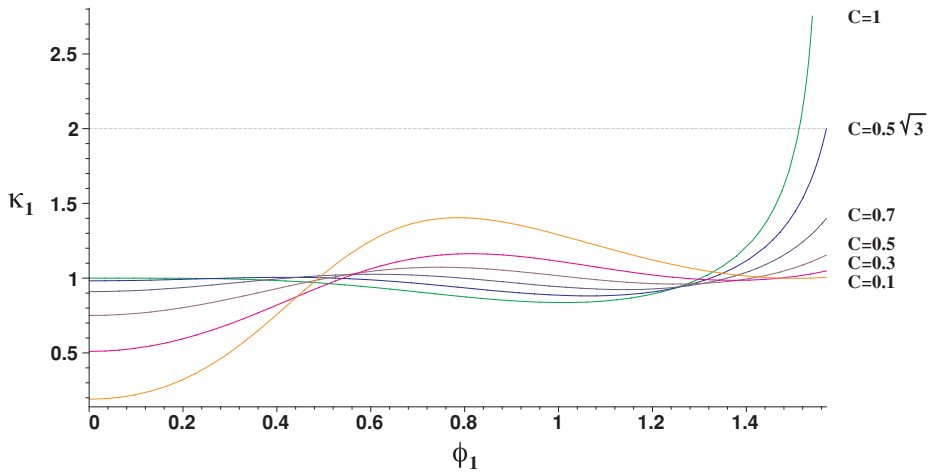

Fig. 3. The curvature κ_1 as function of ϕ_1 for various C.

$$x_2(\phi_2) - x_2(\phi_{20}) = \cot\tilde{\phi}_2 z_2\left(\tilde{\phi}_2\right)\Big|_{\phi_{20}}^{\phi_2} + \int_{\phi_{20}}^{\phi_2} \frac{z_2\left(\tilde{\phi}_2\right)}{\sin^2\tilde{\phi}_2} d\tilde{\phi}_2. \tag{30}$$

Note that the integrals in Eq. (28) and Eq. (30) are hyperelliptic integrals.

We can now see that the curves $\boldsymbol{r}_1(\phi_1)$ and $\boldsymbol{r}_2(\phi_2)$ are described by essentially the same expressions, which implies the following symmetry property: if $\boldsymbol{r}_1(\phi_1)$ is known, then the corresponding second curve $\boldsymbol{r}_2(\phi_2)$ may be obtained by 1) rotating the xy-plane through $\pi/2$ about the axis $y = 1$, $z = 0$ to place $\boldsymbol{r}_1$ into the plane $y = 1$, 2) reflecting the new curve about the yz-plane, and 3) shifting the curve along the line $y = 1, z = 0$ to satisfy the condition of constant distance between the curves. The symmetry property holds true if we consider the entire curves for given C.

In order to find an expression for the curvature κ_1, we again make use of Eq. (26)

$$\begin{aligned}\kappa_1(\phi_1) &= \frac{1}{\sqrt{\left(\frac{dx_1}{d\phi_1}\right)^2 + \left(\frac{dy_1}{d\phi_1}\right)^2}} = \left|\sin\phi_1\left(\frac{dy_1}{d\phi_1}\right)^{-1}\right| \\ &= \frac{\sqrt{1-(C-\cos\phi_1)^2}\left[1-(C-\cos\phi_1)^2\cos^2\phi_1\right]^{3/2}}{\left|1-C^2+\cos\phi_1\left[C+\left(2-\cos^2\phi_1\right)(C-\cos\phi_1)\right]\right|}.\end{aligned} \tag{31}$$

The function in Eq. (31) is singular at $C = 1$, $\cos\phi_1 = 0$ and at $C = 0$, $\cos\phi_1 = 1$. The graph of this function for some values of C is presented in Fig. 3.

As we have seen, for $\phi_1 = \pi/2$, when the curve $\boldsymbol{r}_1$ passes through the plane of the second curve, the last formula reduces to

$$\kappa_1(\pi/2) = \frac{1}{\sqrt{1-C^2}}, \tag{32}$$

which has sense only for $|C| < 1$.

The length of the fragment of the curve with non-vanishing curvature may be found from the quadrature

$$L = \int_{\phi_{10}}^{\phi_{11}} \frac{d\tilde{\phi}_1}{\kappa_1\left(\tilde{\phi}_1\right)}. \tag{33}$$

Assuming both $y'(\phi_1) \geq 0$ and $\sin\phi_1 > 0$, the last expression may be integrated by parts to take the form

$$L = \left.\frac{y_1\left(\tilde{\phi}_1\right)}{\sin\tilde{\phi}_1}\right|_{\phi_{10}}^{\phi_{11}} + \int_{\phi_{10}}^{\phi_{11}} \frac{y_1\left(\tilde{\phi}_1\right)\cos\tilde{\phi}_1}{\sin^2\tilde{\phi}_1}\, d\tilde{\phi}_1. \tag{34}$$

One further improvement can be made. The very formulation of the constrained variational problem Eq. (6) does not guarantee that the solutions found provide the minimal distance between two centreline curves. The conditions Eq. (4) and Eq. (5) only stand for an extremality of the distance. Therefore, we have to consider how to distinguish its minima.

Let $D(\sigma_1, \sigma_2) = \|\boldsymbol{r}_1(\sigma_1) - \boldsymbol{r}_2(\sigma_2)\|^2$ be the squared distance between the points on two curves which are parametrized with σ_1 and σ_2. Then, for the solution of the problem Eq. (6), $(\partial D)/(\partial\sigma_1) \equiv (\partial D)/(\partial\sigma_2) \equiv 0$. Consider a pair of closest points on two curves. Let their parameters be σ_1^*, σ_2^*. Then, for σ_1^*, σ_2^*, the matrix of second derivatives $(\partial^2 D)/(\partial\sigma_i\partial\sigma_j)$, $i, j = 1, 2$, always has one zero eigenvalue corresponding to the closest point parametrization. The positive sign of the second eigenvalue indicates that the distance between two centrelines reaches its minimal value for the closest-point pair with σ_1^*, σ_2^*.

Since we know the explicit parametric expressions for the centreline coordinates Eqs. (20)–(22) or Eqs. (23)–(25), it is easy to compute the second derivatives of the distance D considered as a function of $\sigma_1 = \cos\phi_1$ and $\sigma_2 = \cos\phi_2$ for $\phi_{1,2} \in [0, \pi/2]$. In order that the distance be minimal, the following condition should be satisfied:

$$S(\sigma_1, C) \equiv Tr\left(\frac{\partial^2 D}{\partial\sigma_i\partial\sigma_j}\right)\Bigg|_{\sigma_1+\sigma_2=C} \equiv \frac{\partial^2 D}{\partial\sigma_1^2} + \frac{\partial^2 D}{\partial\sigma_2^2}\Bigg|_{\sigma_1+\sigma_2=C} > 0.$$

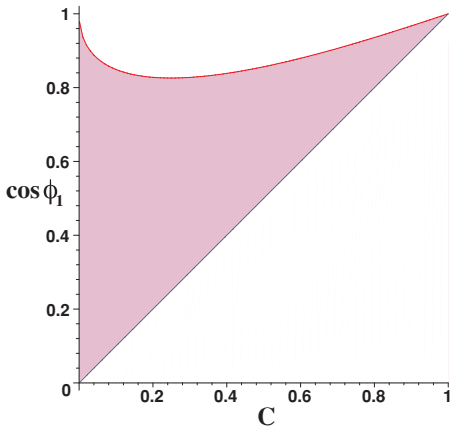

Fig. 4. The region is shaded where the extremal distance between the centrelines is not minimal.

(Here the constraint $\sigma_1 + \sigma_2 = C$ is just Eq. (13).) Thus, an explicit algebraic expression for $S(\sigma_1, C)$ may be obtained. Note that, in contrast to the expressions for the $x_{1,2}$-coordinates, it involves no quadrature. The final form of S is too unwieldy to be presented here, but it may be readily manipulated with the help of a symbolic algebra software like MAPLE to justify the following properties:

1. $S(\sigma_1, \sigma_1) = 0$ for $\sigma_1 \in [0, 1]$,
2. $S(0, C) = 0$ for $C \in [0, 1]$,
3. $S(\sigma_1, C) > 0$ for $\sigma_1 \in [0, 1]$ and $C \in (0, \sigma_1)$,
4. $\lim_{\sigma_1 \to 1} S(\sigma_1, C) = +\infty$ for $C \in (0,1)$.

Properties (2) and (4) suggest that, for every $C \in (0, 1)$, there exists a value $\sigma_1 \in (C, 1)$ such that $S(\sigma_1, C) = 0$. Indeed, numerical computation reveals the second zero-value curve for S in addition to the diagonal (Fig. 4). Therefore, the solutions do not provide the minimal distance if the parameters fall within the shaded region in the figure.

In the next sections we apply the obtained results to the construction of tight shapes of some linked structures. The set of building blocks includes: 1) (contact-free) straight line pieces; 2) circular arcs of unit radius, which are in correspondence with a single point on the other piece; 3) circular arcs of one-half radius (self-contacted pieces); 4) non-straight, non-circular extremal curves as described above.

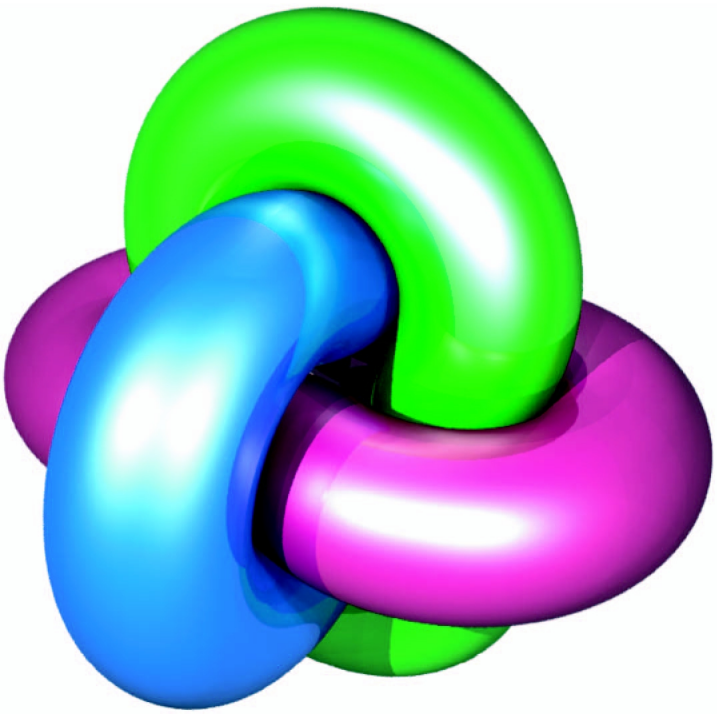

Fig. 5. The piecewise circular approximation of the ideal Borromean rings.

The tight shapes will be built by joining the fragments so that to provide continuity of tangents in the switching points.

3. Tight Borromean Rings

The Borromean rings (Figs. 5 and 6) are made of three parts which are linked in such a way that once any of them is removed, then the other two are not linked (CROMWELL *et al*., 1998). We assume that each ring is actually a closed incompressible tube of the same length and same uniform diameter. The ideal Borromean rings have, by definition, the minimal possible length-to-thickness ratio. In CANTARELLA *et al*. (2002), an approximation of the ideal Borromean rings was proposed. The whole structure was composed of three identical rings each having a plane centreline made of four circular arcs. It is easy to find the length-to-radius ratio for that shape to be $l_{\mathrm{circ}} = 12(\pi + 4\arcsin(\sqrt{7}-1)/4)$.

There are good reasons to believe that the ideal configuration has to be very close to this piecewise circular one. Here we try to improve it by applying the approach developed in the previous section. We assume that all three rings are congruent and have planar centrelines. Moreover, each ring has two orthogonal planes of symmetry, each plane being orthogonal to the centreline plane. In other words, each ring could be made up of four congruent parts. Without loss of generality, the radius of tube may be taken 1/2, in concordance with unit distance between the centrelines $d = 1$.

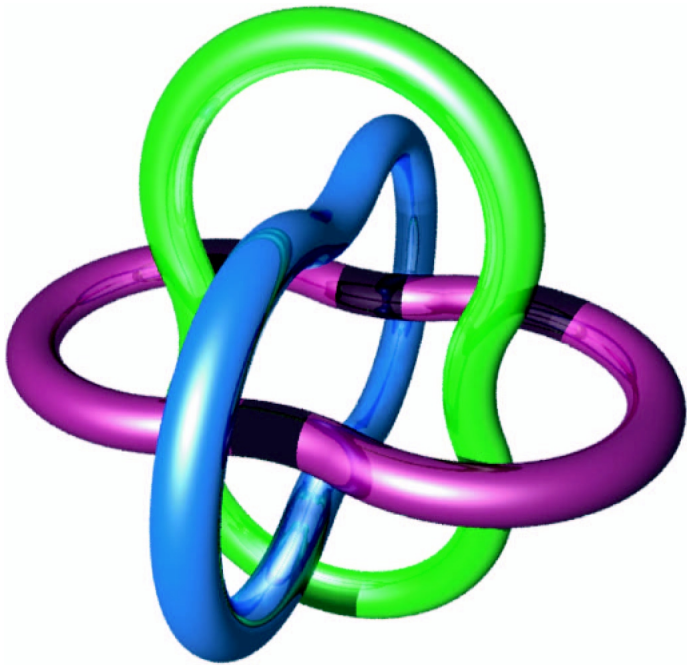

Fig. 6. Borromean rings. The same shape as in Fig. 5 but with smaller thickness of the tube.

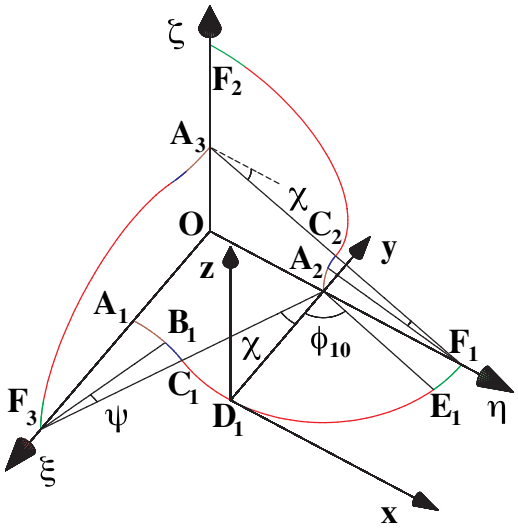

Fig. 7. Construction of tight Borromean rings.

The quarters of three centrelines $A_iB_iC_iD_iE_iF_i$, $i = 1, 2, 3$, are shown in Fig. 7 (not all points are marked). The origin of the reference frame $O\xi\eta\zeta$ is placed in the centre of symmetry of the whole structure, and the coordinate planes coincide with the planes of the centrelines. The origin of the reference frame $Dxyz$ is located in the point $D = D_1 = (1, a, 0)$, $a = OA_i$. At point A_i, the i-th centreline passes orthogonally through the $(i–1)$-th plane (where we identify the zeroth plane with the third one). Suppose $C_1 = (\cos\chi, a - \sin\chi, 0)$ is the first point where the tube 1 comes into contact with the second ring. Thus, C_1 corresponds to A_2. The following piece in the direction of the point D_1 could only be circular of radius 1. Let the circular arc end in some point $E_1 = (\cos\phi_{10}, a + \sin\phi_{10}, 0)$. It could happen that before the point C_1 the tube 1 is either contact-free or it touches the third ring. We continue our consideration under assumption of the second case, though a similar analysis may be done with account for a contact-free segment of positive length, and it may be shown that the shortest centreline is achieved when this straight segment vanishes. Thus, in point C_1 the first tube switches its contact between the third (F_3) and the second (A_2) ones. It means that the distances A_2C_1 and C_1F_3 are unit, and all three points lie on the same straight line as A_2C_1 and C_1F_3 are two perpendiculars to the tangent in the point C_1. For some angle ψ, a fragment of the first tube may have the circular centreline going around point F_3 and the piece A_1B_1 is supposed to be an extremal non-circular solution of continuous contact between the first and the third rings. Thus, we have introduced three unknown angles $\chi \in [0, \pi/2]$, $\psi \in [0, \chi]$ and $\phi_{10} \in [-\chi, \pi/2]$.

The centreline switches from a circular to a non-circular extremal in the point E_1. If we assume that the piece E_1F_1 loses continuous contact with A_2B_2 at some point F_1', then the centreline beginning from F_1' would be either circular (which is evidently impossible) or straight, followed by a circular arc around F_1 with maximal curvature. The second case

may be analyzed in the same way as will be done in the next section for a similar problem. It is shown there that the angle ϕ_{10} should not exceed $\pi/6$, otherwise the configurations would have longer centrelines. It may be demonstrated that, in the case of the Borromean rings, the assembly constraints prevent ϕ_{10} from being less than $\pi/6$. Therefore, we accept that starting at E_1 the centreline proceeds at a constant distance to the piece A_2B_2, and the shape of pieces E_iF_i and $A_{i+1}B_{i+1}$ can be found by applying the formulas developed in the previous section.

The parameters a, χ, ψ and ϕ_{10} should satisfy the following constraints. First of all, it is clear that $a = 2\sin\chi$. We also have

$$a + x_{1F} = 2\cos\chi, \tag{35}$$

where x_{1F} is the x-coordinate of point F_1.

Since the directions of the tangents are determined in the pair of corresponding points E_1 and A_2, we can find the parameter C from Eq. (13): $C = \cos\phi_{10}$. The other pair of corresponding points are F_1 and B_2, but the direction of the continuous tangent at point B_2 is specified by the angle $\chi - \psi$, so we come to the equation $\sin(\chi - \psi) = \cos\phi_{10}$, which means that $\chi + \phi_{10} = \pi/2 + \psi$.

With the last relationship we can eliminate χ and then substitute $a = 2\sin\chi$ into Eq. (35) to obtain

$$x_{1F} = 2[\sin(\phi_{10} - \psi) - \cos(\phi_{10} - \psi)]. \tag{36}$$

By using Eq. (28), we find

$$x_{1F} = \csc\phi_{10} - \int_{\phi_{10}}^{\pi/2} \frac{1 - y_1\left(\tilde{\phi}_1\right)}{\sin^2\tilde{\phi}_1}\, d\tilde{\phi}_1, \tag{37}$$

where y_1 is computed by Eq. (21). Finally, Eq. (36) may be given the form

$$\int_{\phi_{10}}^{\pi/2} \frac{\cos\tilde{\phi}_1}{\sin^2\tilde{\phi}_1} \sqrt{\frac{1 - \left(\cos\phi_{10} - \cos\tilde{\phi}_1\right)^2}{1 - \left(\cos\phi_{10} - \cos\tilde{\phi}_1\right)^2 \cos^2\tilde{\phi}_1}}\, d\tilde{\phi}_1 = \csc\phi_{10} + 2\left[\cos\left(\phi_{10} - \psi\right) - \sin\left(\phi_{10} - \psi\right)\right]. \tag{38}$$

The last integral equation may be considered as a constraint on the values of ψ and ϕ_{10}. It can be solved numerically to obtain a one-parameter family of possible shapes. There is only one branch of solutions in the range $0 < \phi_{10} \le \pi/2$, $\psi \ge 0$. For every configuration, we compute its length-to-radius ratio by using Eqs. (34) and (21). In our case

$$l = 12(4\psi + \pi + 2l_c), \tag{39}$$

where

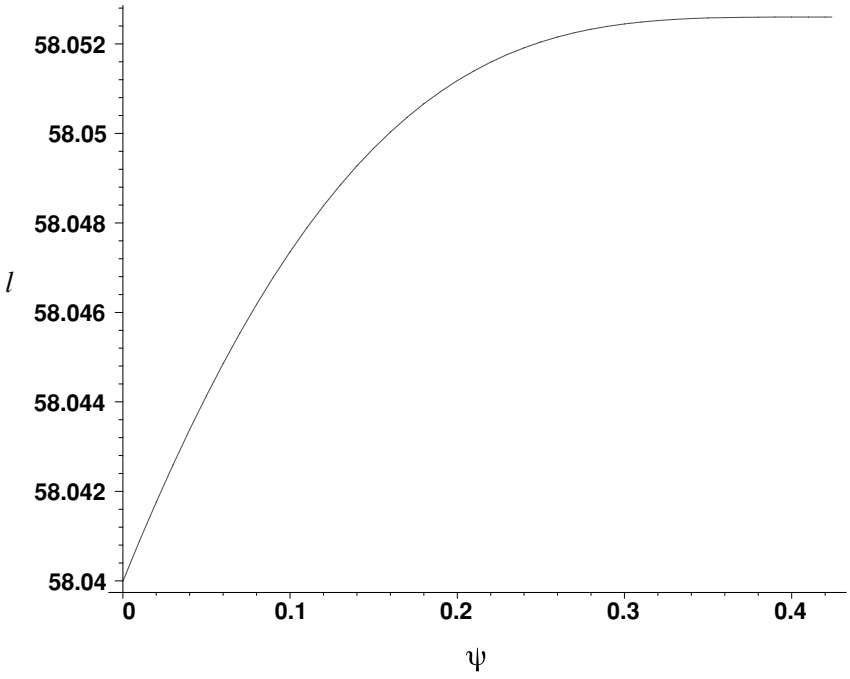

Fig. 8. The length-to-radius ratio l vs. the angle ψ (cf. Eq. (39)).

$$l_c = 2\int_{\phi_{10}}^{\pi/2} \frac{d\tilde{\phi}_1}{\kappa_1\left(\tilde{\phi}_1\right)} = 2\left(\cot\phi_{10} - \int_{\phi_{10}}^{\pi/2} \frac{\left[1 - y_1\left(\tilde{\phi}_1\right)\right]\cos\tilde{\phi}_1}{\sin^2\tilde{\phi}_1} d\tilde{\phi}_1 \right)$$

is the normalized length of extremal arc computed by Eq. (33).

In Fig. 8 the dependence of the length-to-radius ratio is presented as a function of ψ. We see that the tightest shape is achieved for $\psi = 0$, i.e. when the arc B_iC_i disappears. As ψ grows to its maximum $\psi = \chi = \arcsin(\sqrt{7} - 1)/4$, the length-to-radius ratio approaches the limit where there are no non-circular arcs A_iB_i and E_iF_i and $\phi_{10} = \pi/2$.

For the tightest configuration, $\phi_{10} \approx 1.14723118$ (65.73°). The distance OA_i is $a = 2\cos\phi_{10} \approx 0.822026$. The numerical value of the length-to-radius ratio will be $l \approx 58.0399908$. As compared to the "circular" configuration with $l_{\text{circ}} \approx 58.0526017$, the new shape is shorter by $\Delta l = l_{\text{circ}} - 1 = 0.0126109$. (The numerical simulation gives a result which is less optimal than the "circular" one: $l_{120} \approx 58.3052$, due to LAURIE (2002) where each ring was modelled as a 40-gon.)

We see that the difference between the two shapes is so small that it could hardly be visible to the naked eye. Figure 9 shows the actual arrangement of the rings in space. The thickness of the tubes is reduced by half to make the contact line visible. Only two

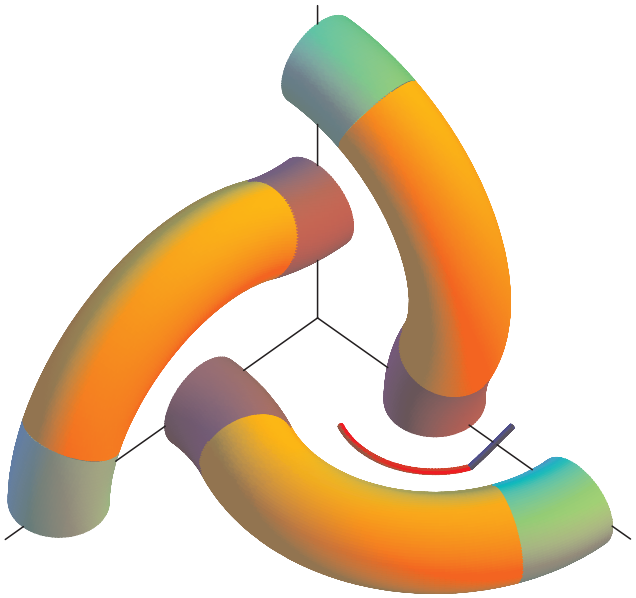

Fig. 9. Tight Borromean rings. One quarter of each ring is shown. Two fragments of the contact line are displayed. The thickness radius of the tubes is set 1/4 instead of 1/2 to make the structure easier to understand.

fragments of the latter are drawn: 1) a circular one formed as the fragment with the centreline $C_1D_1E_1$ goes around the cross-section at point A_2, and 2) the contact curve between the pieces corresponding to E_1F_1 and A_2C_2 (see Fig. 7).

The dependence of the curvature on the angle ϕ_1 is shown in Fig. 10 for the extremal non-circular arc E_iF_i.

4. On the Shape of the Clasped Rope of Minimal Length

As another example we consider the linked structure formed by two pieces of incompressible inextensible rope (Fig. 11). Let us fix the diameter of the cross-section to 1. The entire structure is located between two parallel planes α and β, and each piece of the rope is attached to its own plane at the points $G_1 \in \alpha, H_1 \in \alpha$ and $G_2 \in \beta, H_2 \in \beta$. The straight line segments G_1H_1 and G_2H_2 are orthogonal to each other and they have the same length N, $N \geq 1$. Denote the distance between the parallel planes by M, $M \geq 2$.

We assume that each loop of the rope has a planar centreline and the length of each piece is equal to $L/2$. The problem is to find the shape of the centrelines such that their total length L be minimal. The centrelines should have a continuous tangent everywhere. In fact, we search for a configuration of only one piece of rope because the second one is assumed to have the same geometry due to the symmetry of the problem.

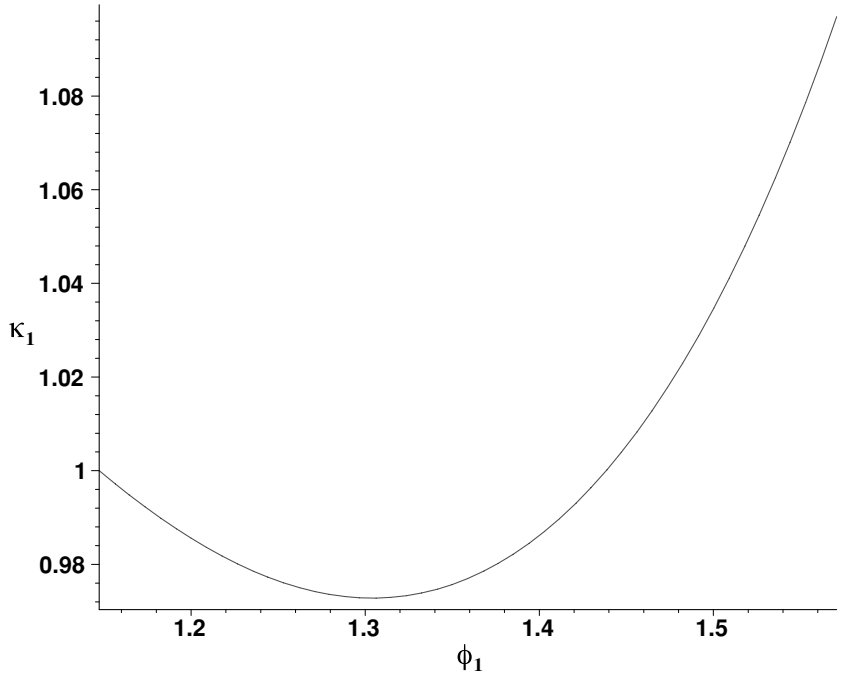

Fig. 10. The curvature $\kappa_1(\phi_1)$ for the centreline fragment E_iF_i.

Figure 12 shows the section of the two clasped ropes by the plane of the first centreline $G_1A_1H_1$. It is symmetric about the axis $K_1A_1 \perp \alpha$, $G_1K_1 = K_1H_1$. A_1 (A_2) is the most distant point on the first (second) centreline from the plane α (β). Denote $x_{1A} = A_1A_2$ and $l_1 = K_1A_2$.

Each half of the centreline includes a straight fragment which does not touch anything, and a curvilinear part which is in contact with the other piece. We concentrate on one half of the 1-st piece $G_1C_1A_1$. G_1C_1 is straight and C_1 is the first point where the contact occurs, i.e. $G_1C_1 \perp C_1A_2$, $C_1A_2 = 1$. Therefore, the entire length of both centrelines is

$$L = 4(L_{GC} + L_{CA}). \tag{40}$$

Let χ be an angle between G_1C_1 and the normal to the plane α. Clearly,

$$L_{GC} = l_1 \sec\chi + \tan\chi. \tag{41}$$

We also have the two relationships:

$$M = 2l_1 + x_{1A} \tag{42}$$

and

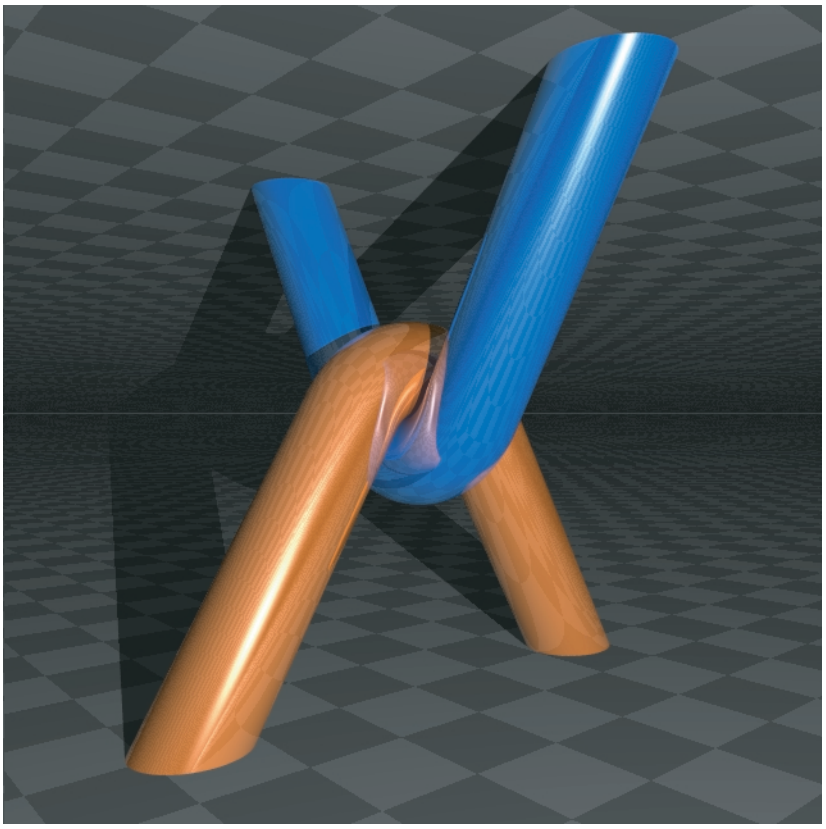

Fig. 11. Two linked pieces of ideal rope are attached to parallel planes.

$$\frac{N}{2} = \sec\chi + l_1 \tan\chi. \tag{43}$$

We continue our analysis assuming that every cross-section along C_1A_1 touches the second rope. Then the non-straight part of the centreline may include two fragments: a circular arc C_1E_1 and the remaining non-circular fragment E_1A_1 (Fig. 13). The piece of rope corresponding to C_1E_1 touches the cross-sectional slice of the second rope with the centre A_2. The part E_1A_1 is in contact with the piece A_2E_2.

Let the location of the point E_1 be specified by the angle ϕ_{10}. Then, since the tangent to the second centreline at point A_2 is orthogonal to the xy-plane, we have from Eq. (13) that $C = \cos\phi_{10}$ and the tangent is continuous in the switching point E_1.

However, the curvature of the centreline is not allowed to be greater than 2, otherwise the tubular neighbourhood of radius 1/2 is not embedded. From Eq. (32) we deduce that, for $\phi_{10} \geq \pi/6$, the curvature at A_1 does not exceed 2. It is also easy to check that the curvature is maximal at A_1 for $\phi_{10} \geq \pi/6$.

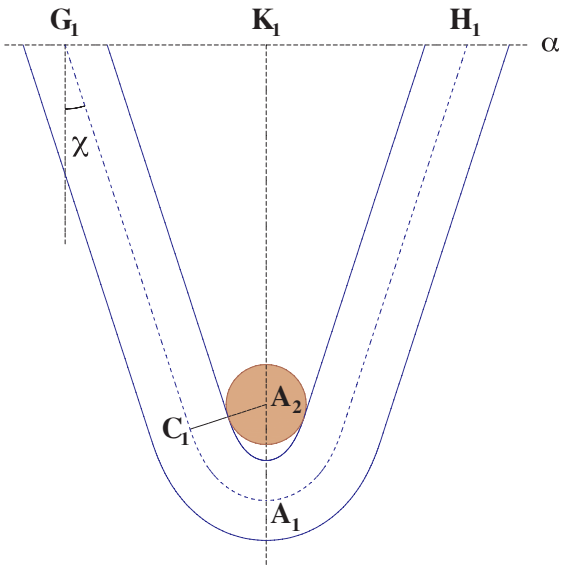

Fig. 12. The central section of the two clasped ropes.

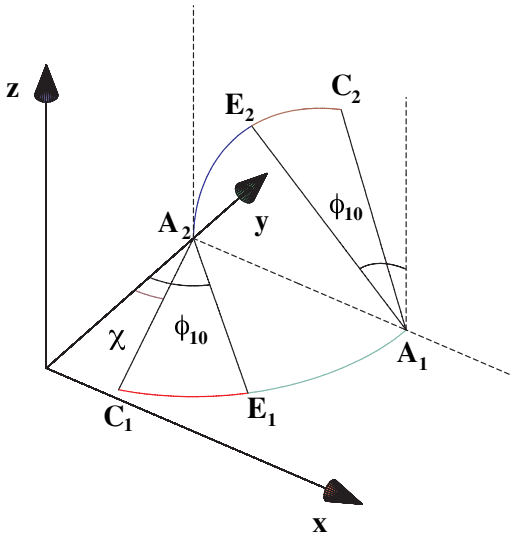

Fig. 13. Construction of tight clasped ropes.

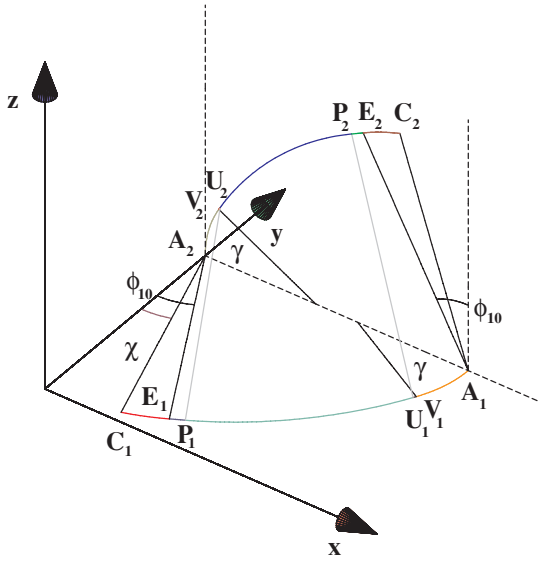

Fig. 14. Construction of tight clasped ropes.

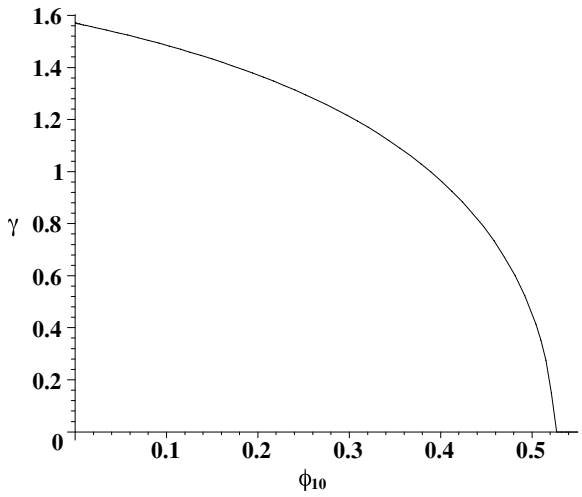

Fig. 15. Construction of tight clasped ropes. The angle γ measures the arc of maximal curvature.

For $\phi_{10} < \pi/6$, the extremal non-circular solution cannot proceed up to the point A_1: it should terminate earlier at a point denoted by U_1 in Fig. 14. For the complementary centreline, this automatically means that the point E_1 would be in correspondence not with A_2 but with another point V_2 which is closer to E_2. Then A_2V_2 would be a circular arc of the

minimal radius 1/2. Since E_1 belongs to the circular arc C_1E_1 of radius 1, it is impossible for E_1V_2 to be orthogonal to both tangents at the points E_1 and V_2. The only possibility to keep a non-zero arc A_2V_2 is to assume that in points E_1 and V_2 the ropes lose contact. More precisely, we introduce two contact-free (hence, straight) fragments E_1P_1 and V_2U_2 such that P_1 is in correspondence with U_2 and the extremal solution describes the fragments P_1U_1 (and U_2P_2).

Let the arc A_1V_1 (and A_2V_2) be measured by angle $\gamma \geq 0$. We denote the straight segments E_1P_1 and V_2U_2 by $\boldsymbol{r}_{|1} = (X_1, Y_1, Z_1)$ and $\boldsymbol{r}_{|2} = (X_2, Y_2, Z_2)$, respectively. Their parametric representation is as follows

$$X_1 = \sin\phi_{10} + t\cos\phi_{10}, \quad Y_1 = 1 - \cos\phi_{10} + t\sin\phi_{10}, \quad Z_1 = 0;$$
$$X_2 = \frac{1-\cos\gamma}{2} + s\sin\gamma, \quad Y_2 = 1, \quad Z_2 = \frac{1}{2}\sin\gamma + s\cos\gamma,$$

where $t \geq 0$, and $s \geq 0$, are parameters. Clearly, the tangents to the curves are continuous at the joining points E_i and V_i.

We are looking for values of $t = t_1$ and $s = s_1$ such that

$$\left\|\mathbf{r}_{|1}(t_1) - \mathbf{r}_{|2}(s_1)\right\| = 1, \quad \frac{d\mathbf{r}_{|1}(t_1)}{dt}\cdot\left(\mathbf{r}_{|1}(t_1) - \mathbf{r}_{|2}(s_1)\right) = 0, \quad \frac{d\mathbf{r}_{|2}(s_1)}{ds}\cdot\left(\mathbf{r}_{|1}(t_1) - \mathbf{r}_{|2}(s_1)\right) = 0. \quad (44)$$

The existence of positive solutions to Eq. (44) provides the possibility to join the straight fragments to the extremal curves without jumps of tangents.

We can express the values t_1 and s_1 from the last two conditions Eq. (44)

$$t_1 = [\cos\gamma(\cos\gamma - 1)/2 + \sin^2\gamma\sin\phi_{10}]\cos\phi_{10}/(1 - \sin^2\gamma\cos^2\phi_{10}),$$

$$s_1 = [\sin\phi_{10} - (\cos\gamma\cos^2\phi_{10} + \sin^2\phi_{10})/2]\sin\gamma/(1 - \sin^2\gamma\cos^2\phi_{10}).$$

Substitution of them into the first condition of Eq. (44) gives an equation for ϕ_{10} and γ which defines implicitly the function $\gamma(\phi_{10})$ (Fig. 15). The value of γ vanishes for $\phi_{10} = \pi/6$, and it increases, as ϕ_{10} becomes smaller.

Now we can compute the length of one half of one centreline. It includes the following components. The length of the circular arc C_1E_1 is simply $L_{CE} = \phi_{10} - \chi \geq 0$ (note that it does not make sense to consider the case $\phi_{10} < \chi$). The length of the remaining part $L_{EA}(\phi_{10})$, $\phi_{10} \in [\chi, \pi/2]$, is the sum $L_{EA} = L_{EP} + L_{PU} + L_{UV} + L_{VA}$, where

$$L_{EP} = \begin{cases} t_1, & \text{if } \phi_{10} < \dfrac{\pi}{6}, \\ 0, & \text{otherwise,} \end{cases} \quad L_{UV} = \begin{cases} s_1, & \text{if } \phi_{10} < \dfrac{\pi}{6}, \\ 0, & \text{otherwise,} \end{cases} \quad L_{VA} = \begin{cases} \gamma/2, & \text{if } \phi_{10} < \dfrac{\pi}{6}, \\ 0, & \text{otherwise,} \end{cases}$$

and L_{PU} may be computed by Eq. (33) with $\phi_{11} = (\pi/2) - \gamma$ and $C = \cos\phi_{10} + \sin\gamma$.

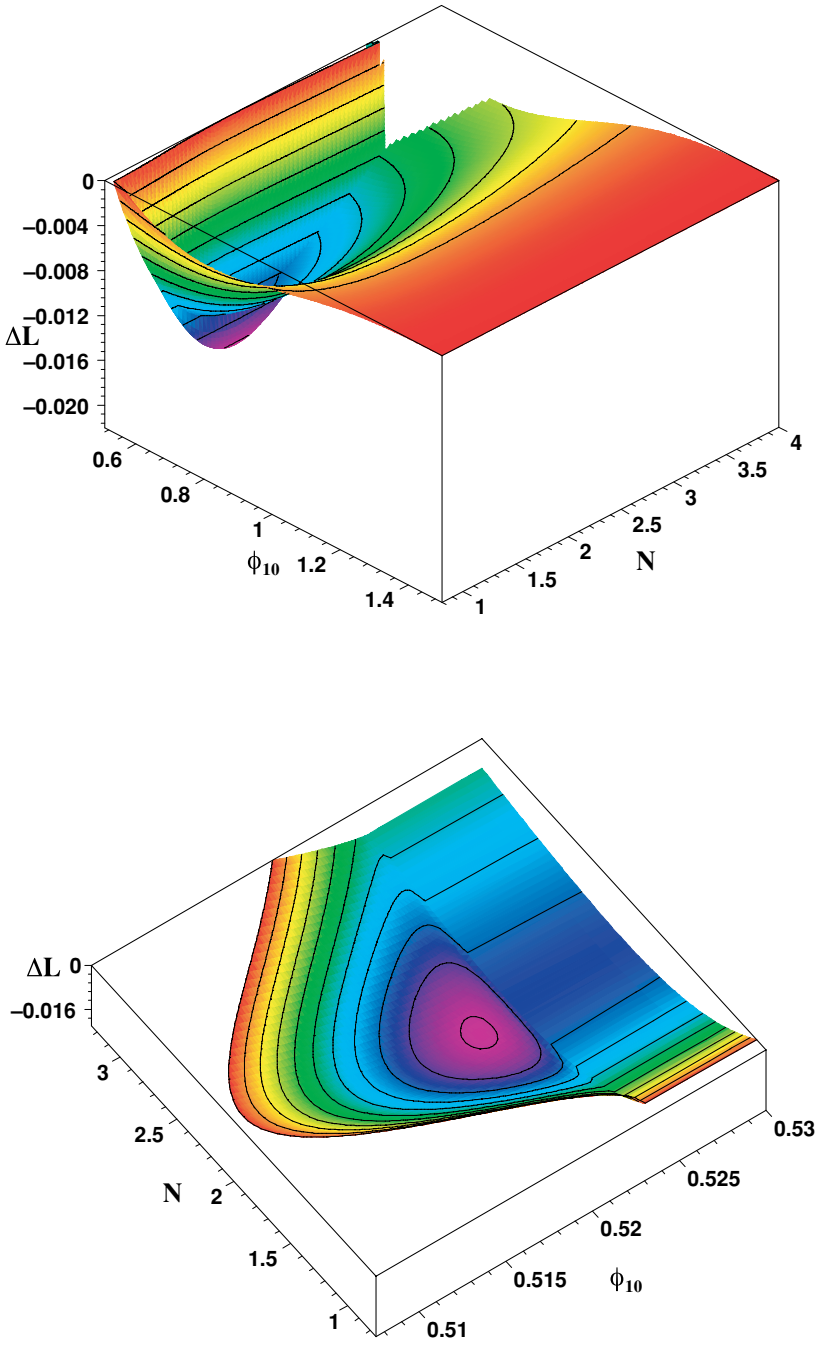

Fig. 16. The gain in length ΔL for $M = 3$ as a function of N and ϕ_{10}.

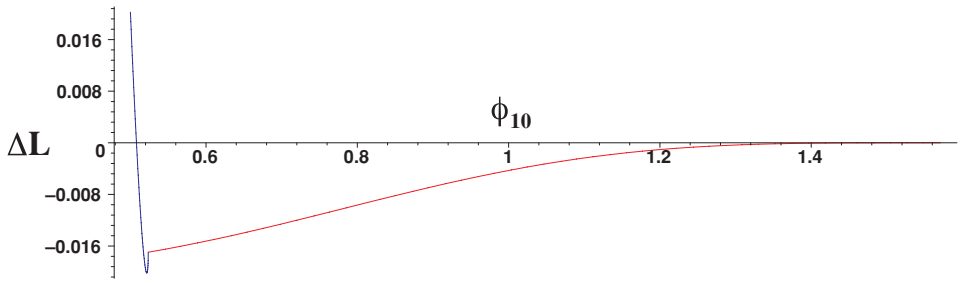

Fig. 17. The gain in length in the parallel case ($N = 2$) as a function of ϕ_{10}.

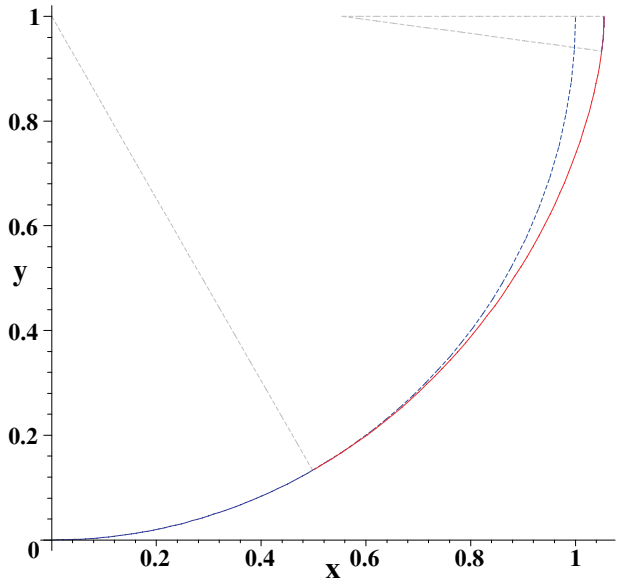

Fig. 18. The centreline of the tight shape compared with the circular arc (dashed) in the parallel case ($N = 2$).

With the help of Eqs. (21) and (28), we find the coordinates of the centrelines; in particular,

$$x_{1A}(\phi_{10}) = \sin\phi_{10} + t_1\cos\phi_{10} + x_1(\phi_{11}) - x_1(\phi_{10}) + s_1\cos\phi_{11} + \frac{1}{2}(1-\sin\phi_{11}). \qquad (45)$$

Now we can express l_1 from Eq. (42), insert it into Eq. (41) and then further substitute L_{GC} into Eq. (40) to obtain

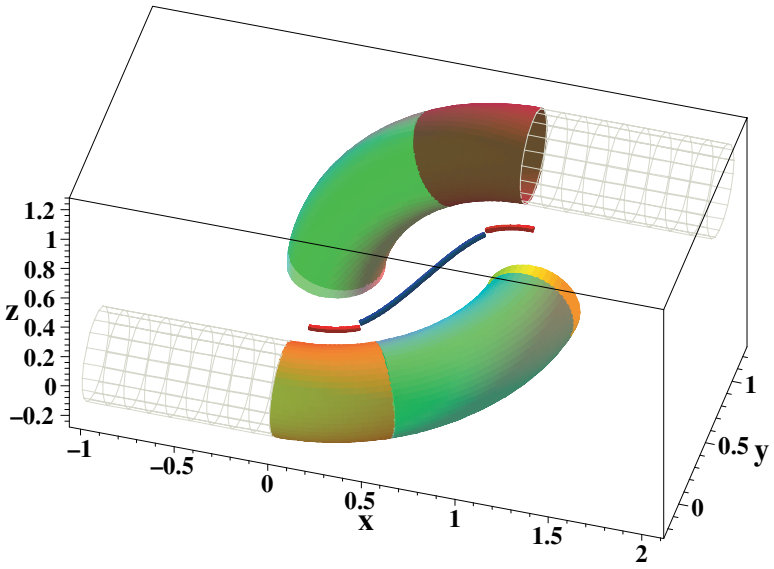

Fig. 19. The tightest clasp in the parallel case ($N = 2$). One half of each piece of rope is shown. Three fragments of the contact line are displayed. The thickness radius of the tubes is drawn as 1/4 instead of 1/2 to make the structure easier to understand.

$$L(M, \chi, \phi_{10}) = 2\{[M - x_{1A}(\phi_{10})]\sec\chi + 2[\tan\chi + \phi_{10} - \chi + L_{EA}(\phi_{10})]\}. \qquad (46)$$

Equation (43) together with Eq. (42) allow us to express the angle χ as a function of M, N and ϕ_{10}:

$$\chi(M, N, \phi_{10}) = 2\arctan\left(\frac{x_{1A}(\phi_{10}) - M + \sqrt{[M - x_{1A}(\phi_{10})]^2 + N^2 - 4}}{N + 2}\right). \qquad (47)$$

Combining Eq. (47) with Eq. (46), we obtain the entire length as a function of M, N and ϕ_{10}. This length can be compared with the one for $\phi_{10} = \pi/2$ which corresponds to the shapes containing no non-circular arc. Figure 16 shows the difference of lengths $\Delta L = L(M, N, \phi_{10}) - L(M, N, \pi/2)$ for fixed $M = 3$. Computations reveal that the absolute minimum is reached for $N = 2$, i.e. for the ropes with parallel straight line parts ($\chi = 0$). In this case, ΔL does not depend on the distance M between the parallel planes. Another property of ΔL is that, for particular N and for $\phi_{10} \geq \pi/6$, the optimal value of ΔL takes place for $\phi_{10}^* = |\chi|$.

Actually, the values of N smaller than 1 mean that the ends of the rope interpenetrate each other. However, we include these values just to demonstrate the global behaviour of ΔL and the connection with the ideal Hopf link which corresponds to $N = 0$, $M = 3$ and $\phi_{10} = \pi/2$.

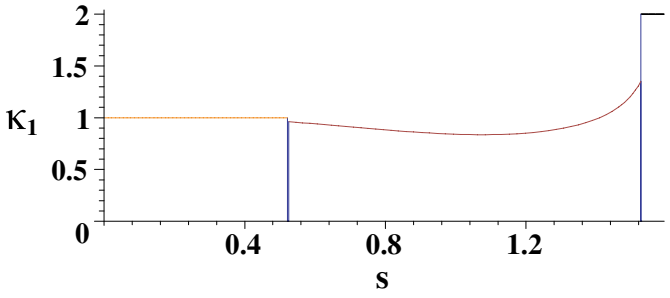

Fig. 20. The curvature $\kappa_1(\phi_1)$ for the segment C_iA_i of the centreline in the parallel case ($N = 2$, $\phi_{10} = \phi_{10}^*$).

Now consider the parallel case in more detail. Figure 17 shows how ΔL changes with ϕ_{10}. The minimal value $\Delta L = -0.0201801598$ is reached for $\phi_{10} = \phi_{10}^* = 0.5216625925$ and $\gamma = 0.1335013510$. Note that the contact-free segments are extremely short: $L_{EP} = 0.0038832246$, $L_{UV} = 0.0002248152$. Figure 18 presents the comparison of the centreline for $\phi_{10} = \phi_{10}^*$ with the circular arc ($\phi_{10} = \pi/2$). We see that their difference is rather small. The contact set is presented in the next Fig. 19. The graph of the curvature of the centreline C_1A_1 is shown in Fig. 20. The curvature is discontinuous because of the presence of straight line segments, it equals 1 at the circular arc C_1E_1, then it jumps to zero for a short interval, after that it behaves smoothly at the segment P_1U_1, then it jumps again for the second short straight line segment, and finally it takes on the maximally allowable value of 2 near the tip point A_1.

5. Periodic Tight Structures

The above solution for the tight clasp of two pieces of the perfect rope can be used to create periodic structures in space. Let us start with the parallel case. As before, we fix the diameter of the cross section to 1. We identify the plane α with the plane β rotated through $\pi/2$ around the common normal to both planes. Then the shape of the linked ropes in case $N = 2$ gives us the periodic chain of period $2M$, $M \geq 2$. It makes little sense to consider such a shape without imposing additional constraints. The linkage density may serve as a good characteristic number to be fixed. We assume first that the chain of n links of the rope connects two parallel planes (Fig. 21). Then the linkage density may be defined as the ratio $\lambda = 2(n - 1)/M$, $\lambda \leq 1$. If $\lambda = 1$ then the shortest chain contains stadium-like rings with circular arcs (CANTARELLA *et al.*, 2002). For smaller values of λ, the shortest configuration includes non-circular curvilinear fragments as described in the previous section. It is easy to see that the parallel clasp problem is the simplest nontrivial case of the chain with $n = 2$. Now we can get rid of the parallel planes at the ends of the chain and consider an infinitely long chain with a specified linking density λ. Its shortest shape is described in exactly the same manner.

It is worth noting that the problem of finding most compact shapes of an one-dimensional periodic structure was considered by PIERAŃSKI (1998) for double-strand

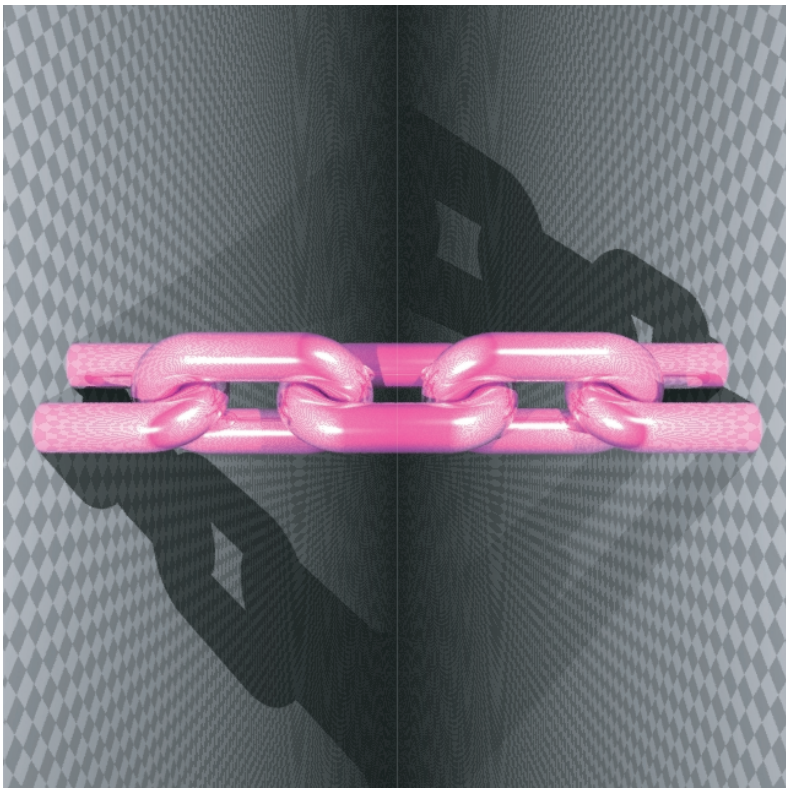

Fig. 21. A tight chain between two parallel walls.

regular helices, and, for the single-strand helix, by MARITAN *et al*. (2000) and by PRZYBYL and PIERAŃSKI (2001). As pointed out by STASIAK and MADDOCKS (2000), in both cases it is necessary to have an additional "compactness condition" on the centreline in order to compensate for the absence of the constraints of closure and knotting. Specification of the linkage density serves the same purpose in the above-described chain.

The rope structures can also be periodic in two dimensions. Again, we start with the case of two clasped perfect ropes and formally set $M = 0$. The last condition means that all four ending points G_i, H_i, $i = 1, 2$, belong to the same plane. Now consider a square of size N, lying in the same plane $\alpha = \beta$, the sides of which are parallel to G_iH_i and contain the end points. The entire plane $\alpha = \beta$ may be covered with square cells $N \times N$, and each cell represents a two-piece clasped rope associated with it. We arrange the ropes in such a way as to make the tangents continuous at the points G_i, H_i. This is accomplished if every two squares having a common side, contain the clasped rope pairs which are reflections of each other in the plane α. Finally, we obtain a two-dimensional periodic structure of periods $2N$ resembling an interwoven textile (Fig. 22). To fix the scale, we set the diameter of the rope's cross section to 1.

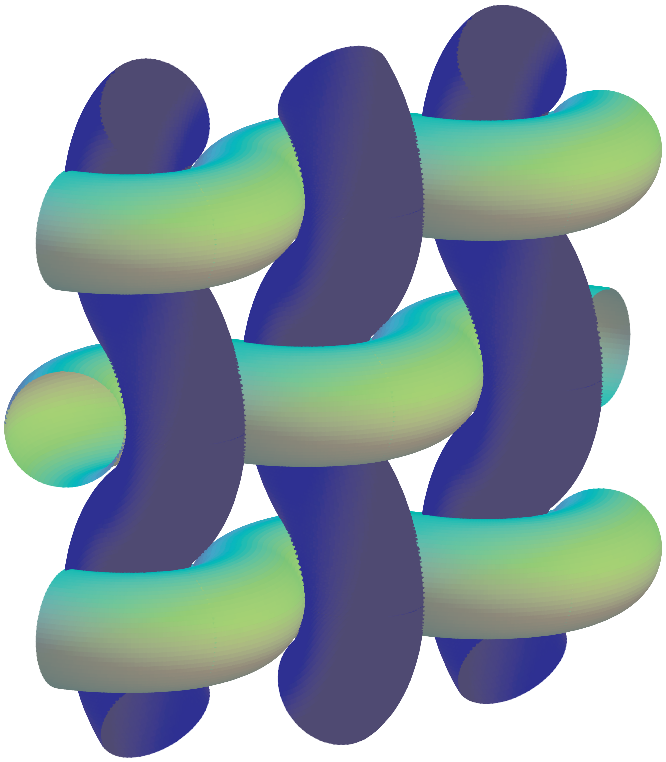

Fig. 22. A two-dimensional periodic tight structure.

Let us consider the shape of the clasp for $M = 0$. Figure 23 represents the difference of the length between the extremal non-circular and circular solutions as a function of the angle ϕ_{10} for various N. For every N, the best result is achieved when ϕ_{10} takes on its minimal possible value $\phi_{10} = \chi$.

The question now arises of how small the semi-period N could be. The smallest N corresponds to the requirement that $C_i \in \alpha$, i.e. $C_i = G_i$. Then $\sin\chi = x_{1A}/2$, $\tan\chi = x_{1A}/N$. Taking $\chi = \phi_{10}$, we come to the equation for ϕ_{10}

$$x_{1A}(\phi_{10}) = 2\sin\phi_{10},$$

which has the solution $\phi_{10} \approx 0.5395100925$. The minimal semi-period is $N = 2\cos\phi_{10} \approx 1.715920915$ and the length of two centrelines per one cell is $L_{\min} \approx 4.163380172$.

We can compare this solution to the shortest shape made up with circular arcs. For the latter, we have $N_{\text{circ}} = \sqrt{3} \approx 1.732050808$, $L_{\text{circ}} = 4\pi/3 \approx 4.188790204$. Therefore, we conclude that the extremal non-circular solution provides the minima both of the cell size N and of the centreline length per period. In that sense this periodic interwoven structure may be called a tight web.

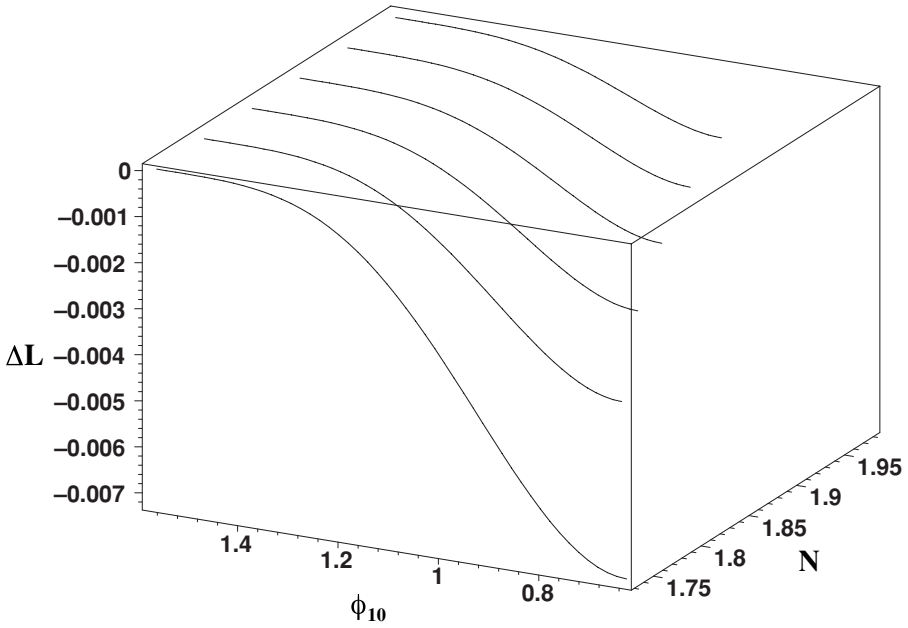

Fig. 23. The gain in length ΔL for $M = 0$ as a function of ϕ_{10} for several values of N.

6. Concluding Remarks

Although we have not proved that the solutions we have found realize ideal shapes (i.e. those with minimal length-to-thickness ratio among all possible configurations of the same topology), the above considerations as well as numerical results suggest that ideal knots and links generically include pieces of rope that contact each other so that the points on the centrelines are in one-to-one correspondence.

It is SULLIVAN who has first pointed to the fact that the shortest shape of two (parallel) clasped ropes is achieved for non-circular centrelines. According to him, there are fragments of a non-zero length in the vicinity of the climax points A_i where the curvature is constant and takes its maximally allowed value of 2. Although his numerical result (see the graph for curvature in SULLIVAN (2003)) looks differently from what is presented in this paper, the difference is likely due to the limited accuracy of numerical computation.

Generally, the problem of the tight clasp of linked ropes is different in the very formulation from the ideal shapes. In the latter, there exist only two natural lengths: the diameter of the rope and its length which means that only its dimensionless ratio is essential for the shape. In the tight clasp problem, we have introduced two more lengths, N and M and, as a consequence, the tight shapes constitute a two-parameter family. We can take another way and specify more constraints in the problem statement. One natural example is the clasp of ropes whose free fragments are constrained to be parallel. If d is the diameter of the cross-section, then the parallelism means the constraint $N = 2d$. As we have seen, the

distance M between the parallel planes does not matter in this particular case. It is possible then to compute the length-to-diameter ratio excluding the long straight pieces of the rope. Thus, we come to the slightly paradoxical concept of the ideal (i.e. having the minimal length-to-diameter ratio) shape of the link consisting of non-closed parts. The parallelism constraint serves as a boundary condition instead of the closure requirement.

In a similar way, the constraint that comes from the periodicity in two dimensions, also replaces the closure property of the components.

The approach presented is developed for the configurations with the centrelines lying in orthogonal planes. It seems to be a straightforward task to adapt the method to centrelines confined to belong to a priori known surfaces. However, it remains unclear how to find those surfaces for ideal knots or links.

Already the special examples (in particular, the Borromean rings) allow us to make a conclusion that the numerical computation of the tightest shapes presents a difficult and delicate problem: in order to obtain a conclusive evidence of some fine features of the extremal shape, the numerical accuracy should be improved by at least two orders. Since the existing algorithms work with discretized centrelines represented as polygonal lines, this means a significant increase of a number of segments that, in turn, will cause an enormous growth of the computational work. A possible way out could be a method that does not use the polygonal approximation. There are good grounds to think that the further development of the variational approach will eventually lead to the design of an efficient and accurate numerical algorithm.

Deep gratitude is expressed to John Maddocks for his support and help with the language and style. The author also thanks Jana Smutny who gave useful feedback on an earlier version of the manuscript. The figures were produced with MAPLE and POV-RAY. Most of the figures appear in colour in the electronic version of the articles.

REFERENCES

CANTARELLA, J., KUSNER, R. and SULLIVAN, J. (2002) On the minimum ropelength of knots and links, *Inventiones Mathematicae*, **150**, 257–286.

CROMWELL, P., BELTRAMI, E. and RAMPICHINI, M. (1998) The Borromean rings, *The Mathematical Intelligencer*, **20**, 53–62.

GONZALEZ, O. and MADDOCKS, J. H. (1999) Global curvature, thickness, and the ideal shapes of knots, *Proc. Natl. Acad. Sci. USA*, **96**, 4769–4773.

GONZALEZ, O., MADDOCKS, J. H., SCHURICHT, F. and VON DER MOSEL, H. (2002) Global curvature and self-contact of nonlinearly elastic curves and rods, *Calculus of Variations and Partial Differential Equations*, **14**, 29–68.

GROSBERG, A. Y., FEIGEL, A. and RABIN, Y. (1996) Flory-type theory of a knotted ring polymer, *Phys. Rev. E*, **54**, 6618–6622.

KATRITCH, V., BEDNAR, J., MICHOUD, D., SCHAREIN, R., DUBOCHET, J. and STASIAK, A. (1996) Geometry and physics of knots, *Nature*, **384**, 142–145.

LAURIE, B. (1998) Annealing ideal knots and links, in *Ideal Knots* (eds. A. Stasiak, V. Katritch and L. H. Kauffman), pp. 42–51, World Scientific.

LAURIE, B. (2002) Knot data and images, web site URL: http://www.links.org/knots/web/knots.html.

LAURIE, B., KATRITCH, V., SOGO, J., KOLLER, T., DUBOCHET, J. and STASIAK, A. (1998) Geometry and physics of catenanes applied to the study of DNA replication, *Biophysical Journal*, **74**, 2815–2822.

LITHERLAND, R., SIMON, J., DURUMERIC, O. and RAWDON, E. (1999) Thickness of knots, *Topology and its Applications*, **91**, 233–244.

MALEVANETS, A. and KAPRAL, R. (1998) Knots in bistable reacting systems, in *Ideal Knots*, (eds. A. Stasiak, V. Katritch and L. H. Kauffman), pp. 234–254, World Scientific.

MARITAN, A., MICHELETTI, C., TROVATO, A. and BANAVAR, J. (2000) Optimal shapes of compact strings, *Nature*, **406**, 287–290.

MOFFATT, H. K. (1990) The energy spectrum of knots and links, *Nature*, **347**, 367–369.

MOFFATT, H. K. (1996) Pulling the knot tight, *Nature*, **384**, 114.

PIERAŃSKI, P. (1998) In search of ideal knots, in *Ideal Knots*, (eds. A. Stasiak, V. Katritch and L. H. Kauffman), pp. 20–41, World Scientific.

PRZYBYL, S. and PIERAŃSKI, P. (2001) Helical close packings of ideal ropes, *The European Physical Journal E*, **4**, 445–449.

STASIAK, A. and MADDOCKS, J. H. (2000) Best packing in proteins and DNA, *Nature*, **406**, 251–253.

STASIAK, A., KATRITCH, V., BEDNAR, J., MICHOUD, D. and DUBOCHET, J. (1996) Electrophoretic mobility of DNA knots, *Nature*, **384**, 122.

SULLIVAN, J. M. (2003) Tight Clasp, *Electronic Geometry Models*, No. 2001.11.001.